



Volume 118

2023

p-ISSN: 0209-3324

e-ISSN: 2450-1549

DOI: <https://doi.org/10.20858/sjsutst.2023.118.6>

Journal homepage: <http://sjsutst.polsl.pl>



**Article citation information:**

Haniszewski, T., Gąska, D., Margielewicz, J., Opasiak, T. Numerical investigations on the dynamic behaviour of a 2-DOF airfoil with application in energy harvesting system. *Scientific Journal of Silesian University of Technology. Series Transport*. 2023, **118**, 77-91. ISSN: 0209-3324. DOI: <https://doi.org/10.20858/sjsutst.2023.118.6>.

**Tomasz HANISZEWSKI<sup>1</sup>, Damian GAŚKA<sup>2</sup>, Jerzy MARGIELEWICZ<sup>3</sup>,  
Tadeusz OPASIAK<sup>4</sup>**

**NUMERICAL INVESTIGATIONS ON THE DYNAMIC BEHAVIOUR  
OF A 2-DOF AIRFOIL WITH APPLICATION IN ENERGY  
HARVESTING SYSTEM**

**Summary.** This article presents the basic airfoil model with two degrees of freedom - the semi-rigid model, where its forced vibrations were considered, and the exciting force is the aerodynamic force, including its periodic changes, that is, gusts. Since the phenomenological model under study has a coupled form, its versions after decoupling are presented, which has an impact on the results of the final research. The airfoil model presented in this way was shown from the application side in the system of a simple energy harvester based on a deformable beam with piezoelectric elements. The result of the simulation tests is a preliminary analysis of the possibility of using the airfoil as a vibration generator for the energy harvesting system. Along with the application of the mechanical part, a numerical simulation of the electrical part was also implemented, related to the transformation of the voltage generated by piezoelectric elements into a constant voltage signal

<sup>1</sup> Faculty of Transport and Aviation Engineering, The Silesian University of Technology, Krasińskiego 8 Street, 40-019 Katowice, Poland. Email: [tomasz.haniszewski@polsl.pl](mailto:tomasz.haniszewski@polsl.pl). ORCID: <https://orcid.org/0000-0002-4241-6974>

<sup>2</sup> Faculty of Transport and Aviation Engineering, The Silesian University of Technology, Krasińskiego 8 Street, 40-019 Katowice, Poland. Email: [damian.gaska@polsl.pl](mailto:damian.gaska@polsl.pl). ORCID: <https://orcid.org/0000-0002-2968-1626>

<sup>3</sup> Faculty of Transport and Aviation Engineering, The Silesian University of Technology, Krasińskiego 8 Street, 40-019 Katowice, Poland. Email: [jerzy.margielewicz@polsl.pl](mailto:jerzy.margielewicz@polsl.pl). ORCID: <https://orcid.org/0000-0003-2249-4059>

<sup>4</sup> Faculty of Transport and Aviation Engineering, The Silesian University of Technology, Krasińskiego 8 Street, 40-019 Katowice, Poland. Email: [tadeusz.opasiak@polsl.pl](mailto:tadeusz.opasiak@polsl.pl). ORCID: <https://orcid.org/0000-0002-0777-2316>

with a connected receiver with power consumption similar to the Atmega microcontroller with battery charging.

**Keywords:** airfoil, simulation, energy harvesting, piezo element, microcontroller

## 1. INTRODUCTION

For several decades, the development of various technologies for obtaining energy not based on fossil fuels has been observed. Since the beginning of this century, energy harvesting has been developing very dynamically, that is, a method of recovering small amounts of energy, but significant for the technique, from sources that normally waste it, for example, vibrations [1, 2], temperature fluctuations [3], air flow [4, 5], solar, etc., which is beneficial in social and ecological aspects. The most frequently developed and tested type of energy harvesting is the recovery of energy from vibrating machine elements; however, in recent years, constantly increasing attention has been given to the air flow, especially considering the flow in ventilation, air conditioning, subway tunnels, etc. The target of energy harvesting is to operate autonomous powered electronic devices, for instance, sensors, but without external power sources.

Wind energy commonly exists in the environment. There is a possibility to use small wind turbines, but in the case of small sensors, it is pointless as traditional wind turbine has a relatively large size and a high cut-in wind speed. The wind-induced vibration energy harvesting is a microenvironmental energy-capturing device [6] designed to harvest beam vibration energy imposed by the air flow by different kinds of energy converters [7] – mostly piezoelectric but also magnetic and others [8]. Piezoelectric transducers have attracted significant interest because they can be used over a wide range of frequencies and are easy to apply [9].

Considering only the energy harvesters whose task is to recover energy from the air flow, we usually deal with a beam at the end of which there is an active element that causes the beam to vibrate [10]. This bluff-body is being placed in a flow field and excited to undergo large oscillations absorbing energy from the air that can be converted into electrical energy using piezoelectric and/or electromagnetic transducers [11]. Aeroelastic phenomena are classified according to their causes and main characteristics. Therefore, we are dealing with flutter [12] when the bluff-body is an airfoil section, vortex-induced vibrations [13, 14], in the case of circular cylinders, galloping [15, 16] for prismatic structures and wake galloping [17, 18] when considering parallel cylinders.

It is important in the design that the energy harvesting takes place for different air flow conditions, including flow velocity variation in analogy to realistic environmental conditions. An airfoil may undergo stall-induced oscillations beyond the critical flutter speed. Such oscillations yield intense periodical motions that can be used to convert the airflow energy into electrical power [19]. The harvester consisted of a rigid airfoil supported by nonlinear flexural and torsional springs under the combination of vibratory base excitations and aerodynamic loadings was considered in [20]. The effects of system parameters on the performance of an energy harvester with three-to-one internal resonance were analyzed in [21]. The research proved that the harvested voltage could be significantly improved in the presence of internal resonance. A modified airfoil-based piezo aeroelastic energy harvester with double plunge degrees of freedom was proposed in [22]. In such systems, there is also the possibility of chaotic movement, which was under consideration in [23]. The investigated airfoil model with higher-order nonlinearities showed multistability with changing airspeed and an infinitely countable

number of coexisting attractors. The airfoil as a bluff-body in energy harvesters was also considered in [24, 25]. The current wind-induced vibration energy harvesters usually work in a relatively narrow wind speed range or have a high cut-in wind speed. In a real application, airflow often has random and unstable characteristics and fluctuation in the wide velocity range.

The aim of this paper is a preliminary analysis of the nonlinear airfoil as a vibration generator for the energy harvesting system together with a numerical simulation of the electrical part related to the transformation of the voltage generated by piezoelectric elements into a constant voltage signal. The most important part of the preliminary research presented in this article is the presentation of the electrical subsystem responsible for the transformation of voltage from alternating AC to constant DC. Also, the relationship of how important it is to achieve a stable waveform of sinusoidal AC voltage generated by the piezoelectric during the operation of the energy harvester was shown.

## 2. PHENOMENOLOGICAL MODEL OF THE CONSIDERED NONLINEAR AIRFOIL SYSTEM WITH SEHS

As shown in the diagram, the system with the energy harvester includes the rigid airfoil model with pitching and plunging degrees of freedom. The piezoelectric coupling is included in the plunging degree of freedom. The equations of motion of the 2 DOF airfoil and energy harvester with wind flow excitation can be represented by equations (1). Symbols  $h$  and  $\alpha$  are plunging and pitching displacements of the presented airfoil,  $c$  is the chord length. The term  $m$  represents the mass parameter of the airfoil. Mass moment of inertia  $I$  is about the elastic axis. Excitation forces and moments are respectively  $L$  and  $M$  that are the aerodynamic lift and moment acting on the selected airfoil. The  $k_h$  and  $k_\alpha$  are the stiffness in the plunging and pitching direction, also  $b_h$  and  $b_\alpha$  are damping parameters.  $R_0$  is the piezoelectric resistance, and  $U_p$  is the voltage generated by the piezo element.  $C_p$  is the capacitance of the piezoelectric material, while  $k_p$  is the electromechanical coupling factor of the piezoelectric material. The data included for the testing model are obtained from publication [12].

$$\begin{aligned} m \frac{d^2 h}{dt^2} + S_\alpha \frac{d^2 \alpha}{dt^2} + k_h h + b_h \frac{dh}{dt} + k_p U_p &= -L \\ S_\alpha \frac{d^2 h}{dt^2} + I \frac{d^2 \alpha}{dt^2} + k_\alpha(\alpha) + b_\alpha \frac{d\alpha}{dt} &= M \\ C_p \frac{dU_p}{dt} + \frac{U_p}{R_0} + k_p \frac{dh}{dt} &= 0 \end{aligned} \quad (1)$$

$$\begin{aligned} b &= 0.135 [m], e = -0.1 [m], m = 12.387 [kg], \alpha_0 = 10 [deg], c_l = 6.28 [-], c_m = \\ &= -0.628 [-], I = 0,065 [kgm^2], S_\alpha = m(x_\alpha b) [kgm], k_h = 2844.4 [N/m], b_h = \\ &= 27,43 [Ns/m], b_\alpha = 0,18 [Nm s/rad], a = -0.6 [-], x_\alpha = 0.2466[-], \rho = \\ &= 1,2255 [kg/m^3], k_{\alpha_0} = 2.82 [Nm/rad], k_{\alpha_1} = 14.1 [Nm/rad^2], k_{\alpha_2} = \\ &= 56.4 [Nm/rad^3], C_p = 72 nF, k_p = 3.985 \cdot 10^{-5} N/V; R_0 = 1 \cdot 10^6 \Omega \end{aligned}$$

The forcing of vibrations in the system presented in (2) is a combination of the lift force and the moment acting on the airfoil with the change of wind speed and its gusts (4) with selected parameters.

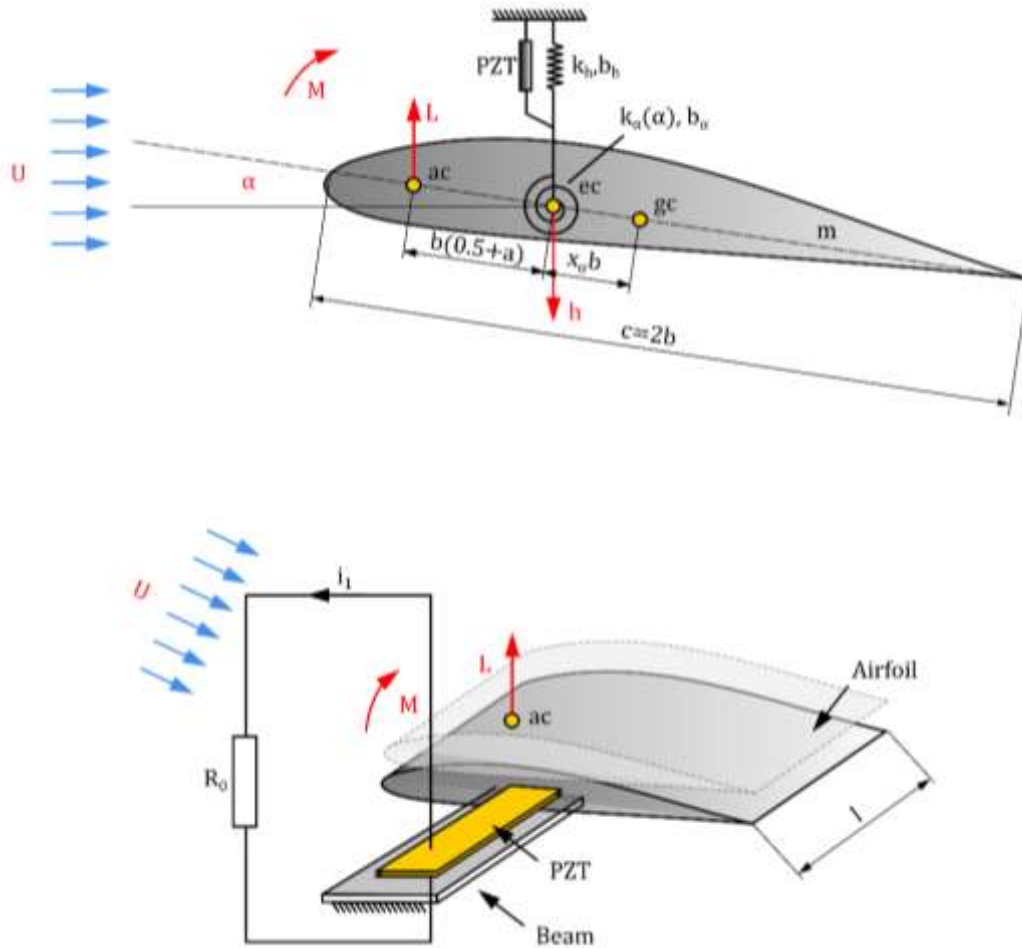


Fig. 1. Physical model of an airfoil with two degrees of freedom

$$\begin{aligned}
 L &= b\rho U^2 \frac{\partial C_{L\alpha}}{\partial \alpha} \alpha \\
 M &= b\rho U^2 \frac{\partial C_{M\alpha}}{\partial \alpha} \alpha \left[ b \left( \frac{1}{2} + a \right) \right]
 \end{aligned} \tag{2}$$

The nonlinearity of the model is implemented through a nonlinear torsional stiffness, which is assumed to be described as a polynomial function (3).

$$k_{\alpha}(\alpha) = k_{\alpha_0} + k_{\alpha_1} \alpha^2 + k_{\alpha_2} \alpha^3 \tag{3}$$

Relationship 4 shows the time course of the wind speed, which is a factor that forces the airfoil structure to vibrate, where  $A_0$  determines the amplitude of a gust of wind,  $\omega_w$  is the frequency of these changes, and  $U_0$  is the base value of the wind speed. The presented dependence allows consideration of the wind gusts or not depending on the adopted parameter  $A_0$ .

$$U = A_0 \cos(\omega_w t) + U_0 \quad (4)$$

As the presented system of differential equations (1) is in coupled form, the system was decoupled and presented in form (6). The obtained equations (1) of the motion of the system are inertia-coupled. The model built directly on their basis will contain algebraic loops on signal lines representing the second derivatives of the generalized coordinates. The standard way to solve the problem of algebraic loops is to break them with a signal delay element. However, this may affect the accuracy of the numerical calculations. The signal delay is a kind of additional damping in the system, which in this case, is difficult to justify physically. Due to the accuracy of numerical calculations, it is advisable to inertia decoupling the system of equations of motion. These equations can be treated as a system of algebraic equations due to the second derivatives of the generalized coordinates. It can be checked (to simplify the work, a symbolic calculator was used) that the determinant of the aforementioned system of algebraic equations will be equal to:

$$\det \begin{bmatrix} m & S_\alpha \\ S_\alpha & I \end{bmatrix} = Im - (m x_\alpha b)^2 \quad (5)$$

Since this determinant is always positive, the system of equations can be solved where finally the uncoupled equations are obtained in the form:

$$\begin{aligned} \frac{d^2 h}{dt^2} &= \frac{\left(-L - k_h h - b_h \frac{dh}{dt} - k_p U_p\right) I - \left(M - k_\alpha \alpha - b_\alpha \frac{d\alpha}{dt}\right) S_\alpha}{Im - S_\alpha^2} \\ \frac{d^2 \alpha}{dt^2} &= \frac{-\left(-L - k_h h - b_h \frac{dh}{dt} - k_p U_p\right) S_\alpha + \left(M - k_\alpha \alpha - b_\alpha \frac{d\alpha}{dt}\right) m}{Im - S_\alpha^2} \quad (6) \\ \frac{dU_p}{dt} &= \frac{1}{C_p} \left(-\frac{U_p}{R_0} - k_p \frac{dh}{dt}\right) \end{aligned}$$

## 2.1. Initial identification of zones that are favourable from the energy harvesting approach

The bifurcation diagrams are aimed at presenting the relationship between the value of the voltage generated by the piezoelectric element and the spectrum of changes in the amplitude of the excitation, which in this case, is the amplitude of changes in wind speed.

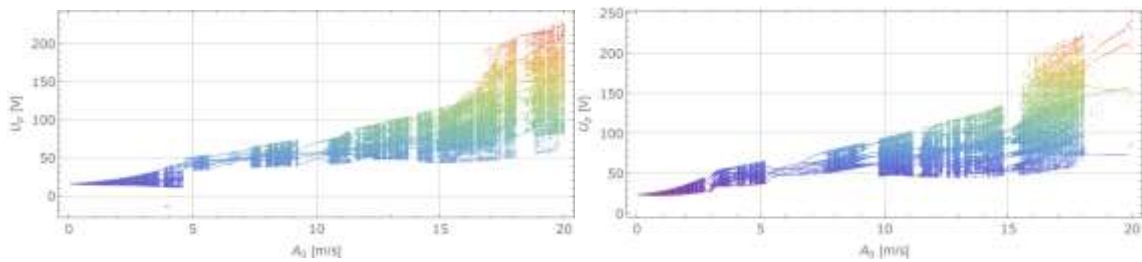


Fig. 2. Bifurcation diagram for wind speed 12, 14 m/s as a function of wind gust amplitude in the range of 0-20 m/s

The diagrams presented in Figures 2, 3, and 4 show 2400 simulations for changes in the input amplitude  $A_0$  from 0 to 20 m/s, assuming two basic wind speeds, that is,  $U_0$ , 12 and 14 m/s, where the frequency of changes  $\omega_w$  was fixed on 10 rad/s. Speeds in the range of 12-14 m/s have been selected because these are critical values responsible for the resonance zone of the system. Based on the bifurcation diagrams presented in Figures 2-4, the cases of the energy harvester's forcing were selected considering the possible ranges of wind velocity and gust amplitudes related to the elastic properties of the material, aimed at excitation of the energy harvesting system. For the cases presented in Table 1, simulations of the system from Figure 1 were performed in the form of oscillograms showing the displacement and velocity of selected airfoil degrees of freedom, that is, vertical and torsional vibrations and the voltage generated on the electrodes of the piezoelectric element being part of the flexible beam on which the airfoil was attached. As observed in the figures created from the numerical simulations (Figure 5), the vertical vibrations of the airfoil reach the limit values in the range of -0.028 to 0.04 m for wind speed 12 m/s and -0.043 to 0.057 m for speed 14 m/s.

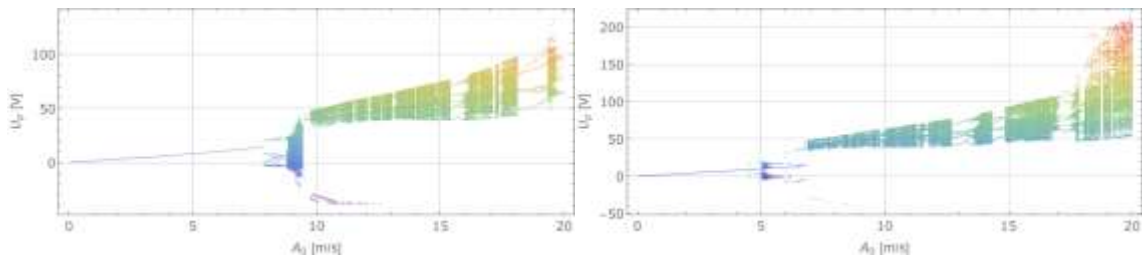


Fig. 3. Bifurcation diagram for wind speed 8, 10 m/s as a function of wind gust amplitude in the range of 0-20 m/s

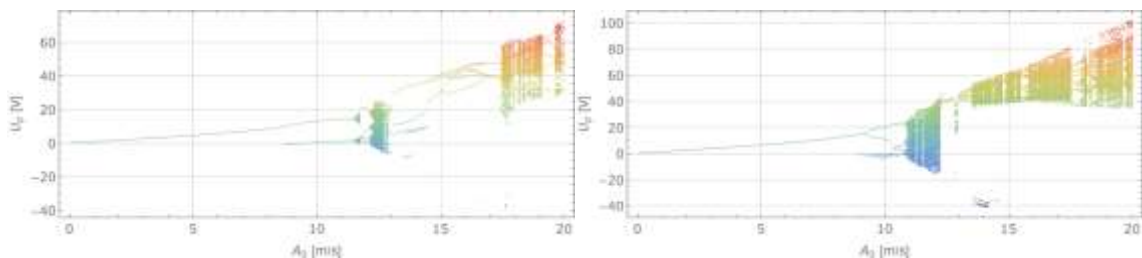


Fig. 4. Bifurcation diagram for wind speed 4, 6 m/s as a function of wind gust amplitude in the range of 0-20 m/s

Tab. 1

Table with calculation cases for selected values based on the bifurcation diagrams (Figures 2-4)

1	$U_0 = 12 \text{ m/s}$	$A_0 = 0 \text{ m/s}, \omega_w = 0 \text{ rad/s}$
	$U_0 = 14 \text{ m/s}$	
2	$U_0 = 12 \text{ m/s}$	$A_0 = 1 \text{ m/s}, \omega_w = 10 \text{ rad/s}$
	$U_0 = 14 \text{ m/s}$	
3	$U_0 = 12 \text{ m/s}$	$A_0 = 3 \text{ m/s}, \omega_w = 10 \text{ rad/s}$
	$U_0 = 14 \text{ m/s}$	

The speed of vertical vibrations is correspondingly -0.6 to 0.6 m/s for wind speed 12 m/s and for 14 m/s appropriately -0.9 to 0.95 m/s. In the case of torsional vibrations, the values of airfoil deflection (torsional vibrations around the beam axis) for wind speed are 12 m/s from -0.92 to 0.56 rad and for 14 m/s appropriately -0.94 to 0.68 rad. The speed of torsional vibrations is within the range -13.12 for 11.55 rad/s for 12 m/s, and wind speed of 14 m/s takes the values of -0.9 to 0.95 m/s. Noticeably, increasing the wind speed by 2 m/s causes an increase in the amplitude of vertical vibrations responsible for the beam deflection with the piezoelectric element, thus, generating higher voltage values, where the peak-to-peak voltage for the wind speed of 12 m/s is 30.61 V and for 14 m/s, it is the value of 47.12 V.

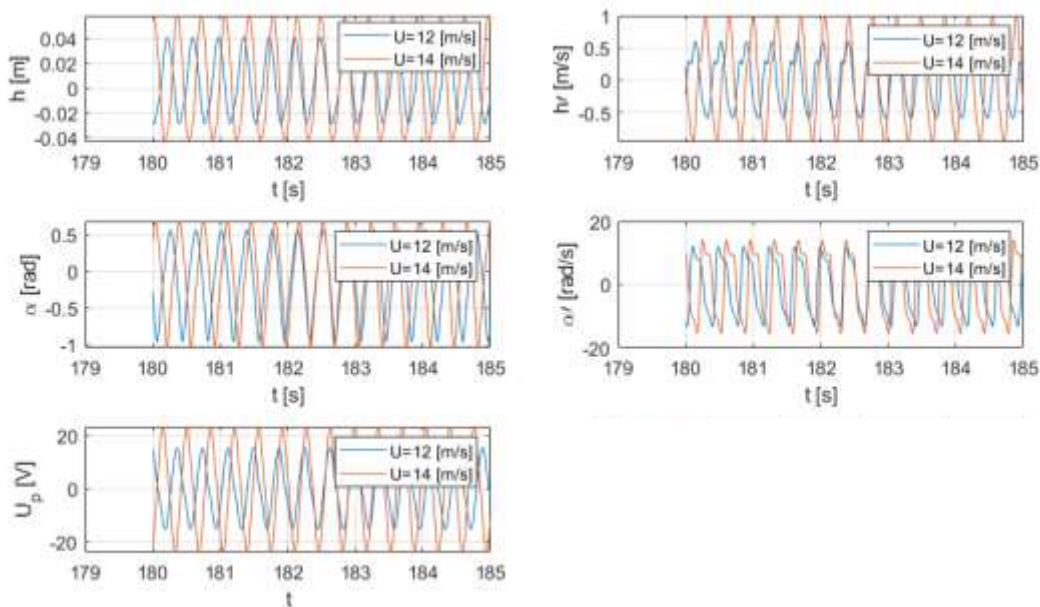


Fig. 5. Results of the simulation tests for two wind speeds, 12 and 14 m/s, no gusts

According to the adopted plan of excitations applied to the airfoil model (Table 1), the second option is to additionally apply the effect of a gust of wind with an amplitude of 1 and 3 m/s and a frequency of 10 rad/s. As can be seen in Figures 6 and 7, the amplitude of vertical vibrations reaches its maximum values in the range from -0.1 to 0.1 m for a wind speed of 14 m/s and a gust with an amplitude of 3 m/s, thus, giving the highest peak voltage value of 51 V.

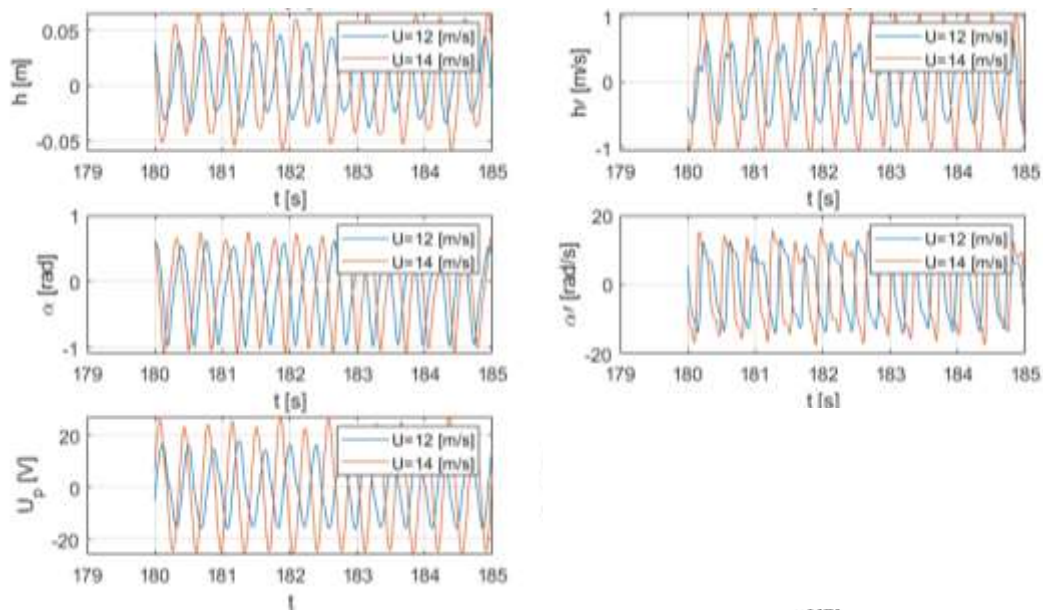


Fig. 6. Results of the simulation tests for two wind speeds, 12 and 14 m/s, a gust of wind with an amplitude of 1 m/s and the excitation frequency of 10 rad/s

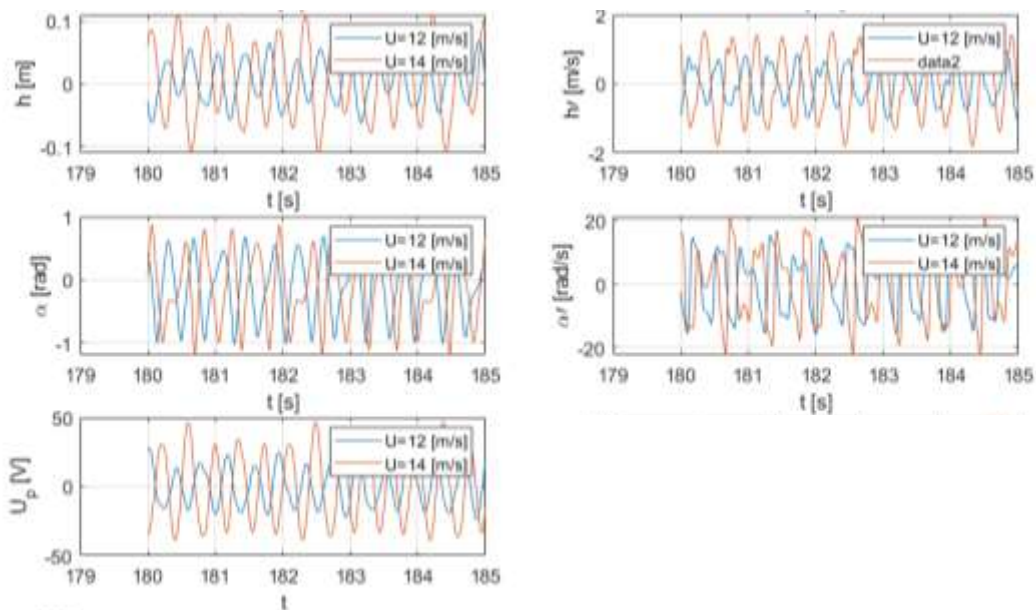


Fig. 7. Results of the simulation tests for two wind speeds, 12 and 14 m/s, a gust of wind with an amplitude of 3 m/s and the excitation frequency of 10 rad/s

For the model under consideration, the negative effect of the gusts is a significant increase in the amplitude of torsional vibrations to the value of about 1 rad, which will contribute to the rapid destruction of the system. It should also be noted that the proposed model does not consider the deformations resulting from torsional vibrations, and the voltage values are obtained only based on the vertical vibrations of the airfoil, that is, they are related to the resulting deflected form of the beam. The speed of the end of the piezoelectric beam is not without significance here, as it, together with the deflection, is responsible for the value of

the obtained voltage. High values of the vertical vibration velocities of the airfoil can be observed when the wind gust is used; these velocities range from -1.73 to 1.48 m/s, and thus, contribute to the generation of the highest peak-to-peak voltage values.

**2.2. Energy acquired - the efficiency of the solution for recovering energy from mechanical vibrations**

In Figure 8, the proposed electronic system is presented, enabling the conversion of the alternating voltage generated by the piezoelectric to a constant value of a specific level. The circuit consists of a full-wave rectifier based on rectifying diodes and a filter capacitor to smooth the DC voltage. Then, to regulate the voltage and ensure the situation of one-way power flow, a buck-converter controlled by the PWM signal and a diode were used to obtain a voltage in the range of 3-4 V at the output, needed to power the microcontroller.

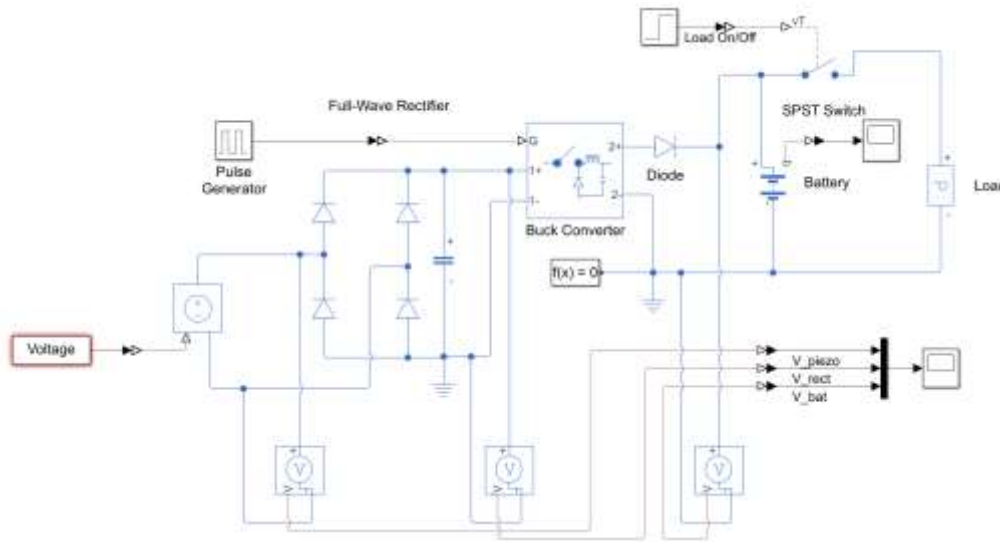


Fig. 8. Voltage transformation system

The pulse generator controls the buck-converter in an open loop with a fixed switching frequency and a defined duty cycle. The energy harvester system initially charges the battery, where after 5 seconds, a receiver with a power of 20 mW and a voltage of 3.3 V is connected to the circuit.

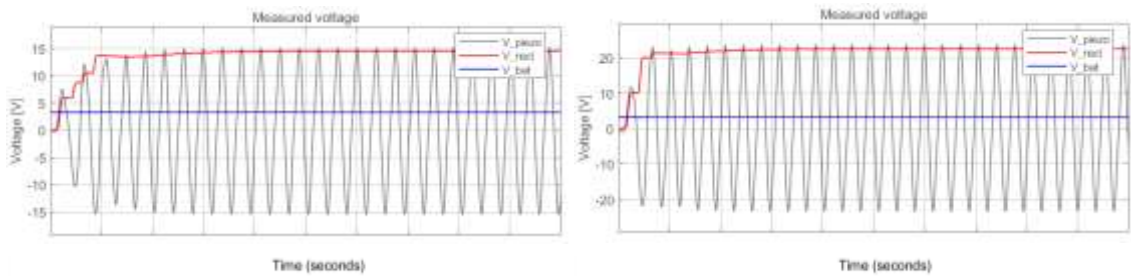


Fig. 9. Results of the simulation tests for a constant wind speed of 12 and 14 m/s

At the input of the system (Figure 8), the voltage generated based on numerical simulations carried out on the tested object was applied. As a result of the conducted conversion of the voltage generated by the energy harvester system into DC voltage, a series of time waveforms was obtained, in the form of voltages, obtained power and the battery charging curve.

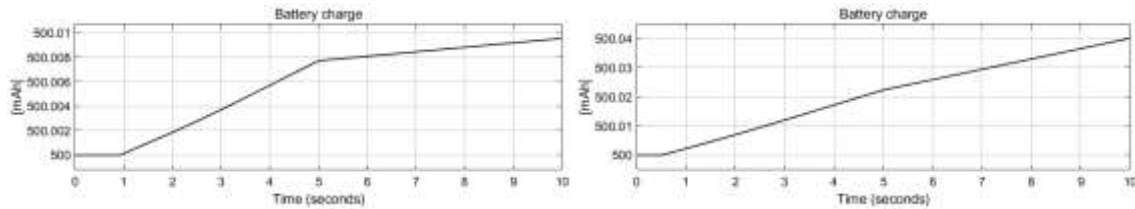


Fig. 10. Time course of battery charging for constant wind speed, 12 and 14 m/s

Figures 9, 12, and 15 show the time history of the voltage generated by the piezoelectric, after rectification by the full-wave rectifier, and the voltage decreased to the desired value for the batteries. Observably, depending on the applied excitation, the values of the voltage generated by the piezoelectric differ given the vibration amplitude and the speed of the vibrating beam, changing from 14.8 to 23.1 V for no gust of wind, 15.8 to 24.6 V for gusts by the amplitude of 1 m/s and 27.5 to 46.3 V for gusts of the amplitude of 3 m/s.

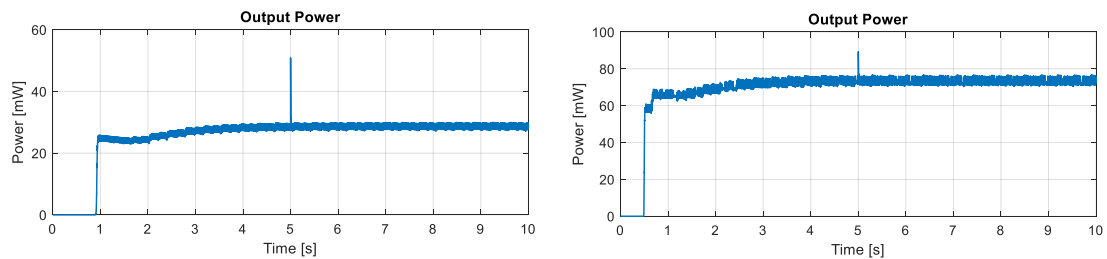


Fig. 11. Results of simulation tests, for constant wind speed, 12 m/s, where output power at final time = 27.86 mW, and 14 m/s, where output power at final time = 72.03 mW

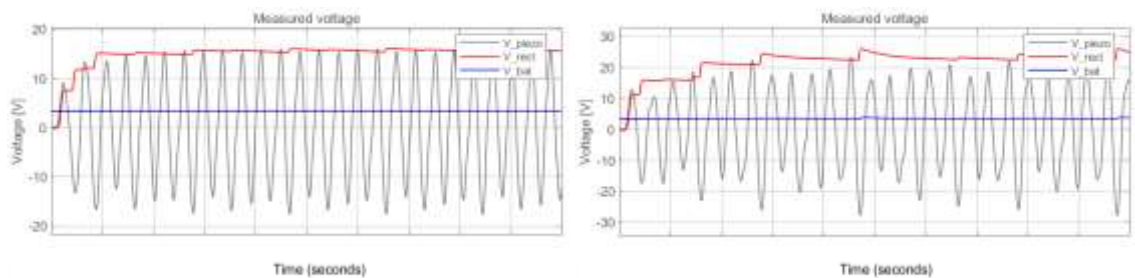


Fig. 12. Results of the simulation tests for wind speed 12 m/s,  
a gust of wind with an amplitude of: a) 1 m/s,  
b) 3 m/s for the frequency of changes in the gust amplitude 10 rad/s

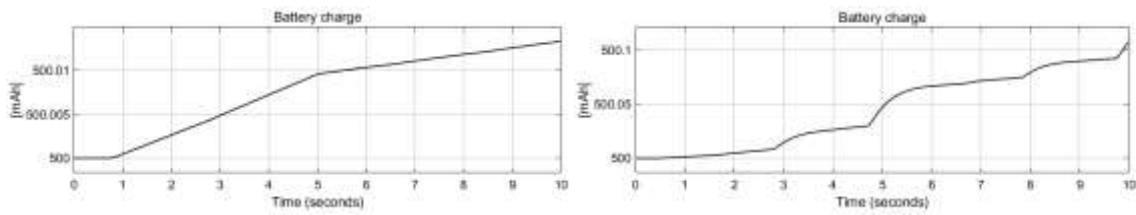


Fig. 13. Time course of battery charging for wind speed 12 m/s, a gust of wind with amplitude: a) 1 m/s, b) 3 m/s for the frequency of changes in the gust amplitude 10 rad/s

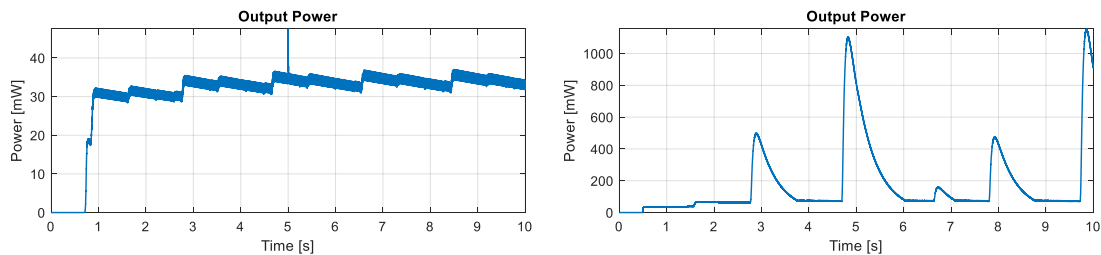


Fig. 14. Results of the simulation tests, for wind speed, 12 m/s, a gust of wind with amplitude: a) 1 m/s where output power at final time = 33.6063 mW, b) 3 m/s where output power at final time = 911.2049 mW for frequency variation of the blast amplitude 10 rad/s

Figures 10, 13, and 16 show the battery charging curves, where for almost every case of extortion, the curve breaking point is characteristic, related to the inclusion of a 20 mW load in the system. The highest charging capacity was obtained for the case of forced wind gusts with an amplitude of 3 m/s, where the charging value closed at 2 mAh in 10 s, giving theoretically 720 mAh charging in one hour, assuming simultaneous operation of the loading device. Charts 11, 14, and 17 present the time history of the power obtained for the tested energy harvester. In the case of no gust, for both 12 and 14 m/s wind speed, constant power values in the range of 27-72 mW were obtained. The use of gusts of wind increases the power generated by the piezoelectric; however, these are only moments reaching the peaks of 15.000 mW.

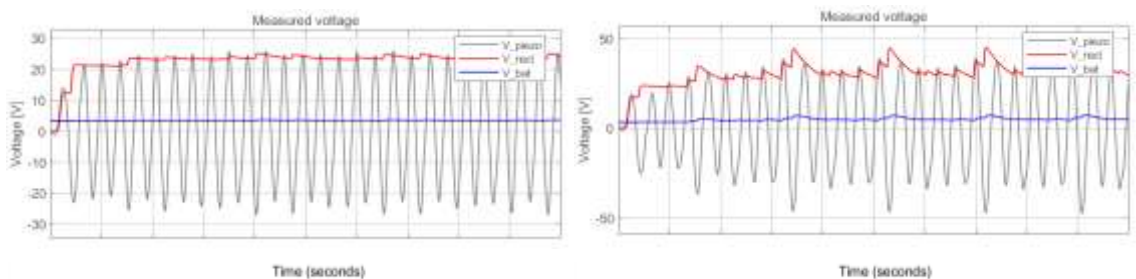


Fig. 15. Results of the simulation tests, for a wind speed of 14 m/s, a gust of wind with an amplitude of: a) 1 m/s, b) 3 m/s, and the excitation frequency of 10 rad/s

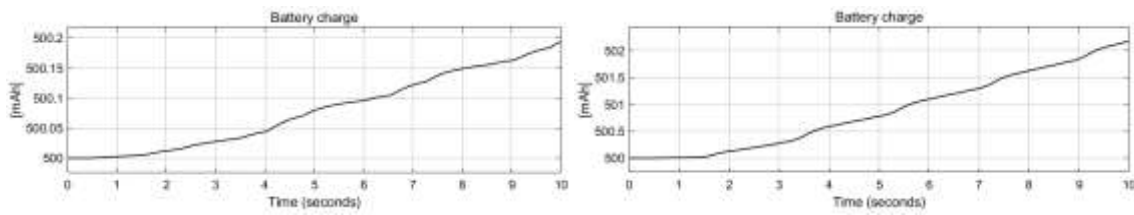


Fig. 16. Time course of battery charging for a wind speed of 14 m/s, a gust of wind with an amplitude of: a) 1 m/s, b) 3 m/s for the frequency of changes in the amplitude of the gust 10 rad/s

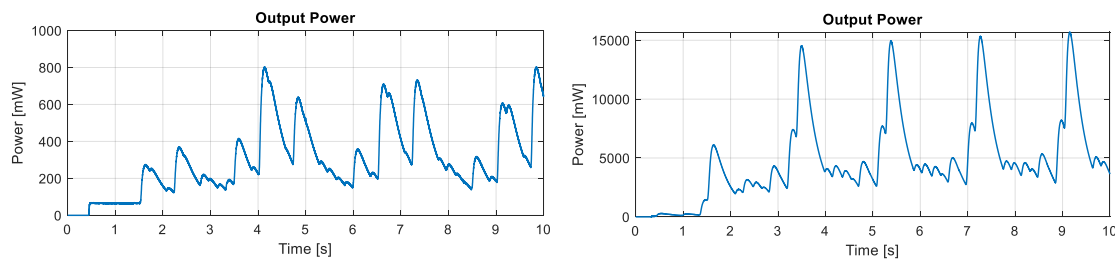


Fig. 17. Results of the simulation tests for a wind speed of 14 m/s, a gust of wind with an amplitude of: a) 1 m/s, b) 3 m/s and the excitation frequency of 10 rad/s, output power at final time = 641.0324 mW and output power at final time = 3639.8759

The average maximum value for the obtained waveforms with an amplitude of 3 m/s is 7800 mW, with the indication that these values are obtained for large deformations of the beam, which should not be the case with the actual system. According to the data obtained from bifurcation diagrams, voltages of the order of 1000 V can be obtained; however, the vibration amplitudes of the beam with the piezoelectric element reach values only possible in theory due to the exceeding of the achievable limit stresses and deformations already beyond the elastic range, thus, leading to the immediate destruction of the device.

### 3. CONCLUSIONS

The presented phenomenological model of a simple energy harvester based on airfoil vibrations, with two degrees of freedom, shows features that allow its use in energy harvesting systems. Nevertheless, it requires a special design due to the high vibration amplitudes. According to the adopted plan of excitations applied to the airfoil model (Table 1), with the addition of the influence of the wind gust, it can be observed that the amplitude of vertical vibrations reaches its maximum values in the range from -0.1 to 0.1 m for a wind speed of 14 m/s and a gust amplitude of 3 m/s, thus giving the highest peak-to-peak voltage of 51V. For the model under consideration, the negative effect of the gusts is a significant increase in the amplitude of torsional vibrations to the value of about 1 rad, which will contribute to the rapid destruction of the system. Further, it should be noted that the proposed model does consider the deformations resulting from torsional vibrations, and the voltage values are obtained only based on the vertical vibrations of the airfoil, that is, they are related to the resulting deflected form of the beam, which should be considered in future research also on a real object. The speed of the end of the piezoelectric beams is not without significance here, as it, together with

the deflection, is responsible for the value of the obtained voltage. High values of the vertical vibration velocities of the airfoil can be observed in the case of blasts. It should also be remembered that it is necessary to obtain a stable sinusoidal waveform of voltage changes, otherwise, the energy gain of the solution will be lower, which is associated with the transformation of the alternating signal into a constant one, where there are losses when passing through the rectifier system and regulating the voltage supplied to the receiver in the form of a battery that is charged by mechanical vibration. An important fact is also to carry out the necessary tests related to the fatigue strength of the proposed solution, aimed at estimating the lifetime of the energy harvesting system presented in this way.

## References

1. Litak Grzegorz, Jerzy Margielewicz, Damian Gąska, Piotr Wolszczak, Shengxi Zhou. 2021. "Multiple Solutions of the Tristable Energy Harvester." *Energies* 14(5): 1284. ISSN: 1996-1073. doi:10.3390/EN14051284.
2. Lan Chunbo, Weiyang Qin. 2017. "Enhancing Ability of Harvesting Energy from Random Vibration by Decreasing the Potential Barrier of Bistable Harvester." *Mechanical Systems and Signal Processing* 85: 71-81. ISSN: 0888-3270. DOI: 10.1016/j.ymsp.2016.07.047.
3. Madruga Santiago. 2021. "Modeling of Enhanced Micro-Energy Harvesting of Thermal Ambient Fluctuations with Metallic Foams Embedded in Phase Change Materials." *Renewable Energy* 168: 424-437. ISSN: 0960-1481. DOI: 10.1016/J.RENENE.2020.12.041.
4. Abdelkefi Abdessattar. 2016. "Aeroelastic Energy Harvesting: A Review." *International Journal of Engineering Science* 100: 112-135. ISSN: 0020-7225. DOI: 10.3390/EN14051284.
5. Wang Junlei, Linfeng Geng, Lin Ding, Hongjun Zhu, Daniil Yurchenko. 2020. "The State-of-the-Art Review on Energy Harvesting from Flow-Induced Vibrations." *Applied Energy* 267: 114902. ISSN: 0306-2619. DOI: 10.1016/J.APENERGY.2020.114902.
6. Lee Yin Jen, Yi Qi, Guangya Zhou, Kim Boon Lua. 2019. "Vortex-Induced Vibration Wind Energy Harvesting by Piezoelectric MEMS Device in Formation." *Scientific Reports* 9(1): 1-11. ISSN: 2045-2322. DOI: 10.1038/s41598-019-56786-0.
7. Zhao Liya, Yaowen Yang. 2018. "An Impact-Based Broadband Aeroelastic Energy Harvester for Concurrent Wind and Base Vibration Energy Harvesting." *Applied Energy* 212: 233-243. ISSN: 0306-2619. DOI: 10.1016/J.APENERGY.2017.12.042.
8. Tan Ting, Lei Zuo, Zhimiao Yan. 2021. "Environment Coupled Piezoelectric Galloping Wind Energy Harvesting." *Sensors and Actuators A: Physical* 323: 112641. ISSN: 0924-4247. DOI: 10.1016/J.SNA.2021.112641.
9. Toroń Bartłomiej, Krystian Mistewicz, Marcin Jesionek, Mateusz Kozioł, Maciej Zubko, Danuta Stróż. 2022. "A New Hybrid Piezo/Triboelectric SbSeI Nanogenerator." *Energy* 238: 122048. ISSN: 0360-5442. DOI: 10.1016/J.ENERGY.2021.122048.
10. Litak Grzegorz, Bartłomiej Ambrozkiwicz, Piotr Wolszczak. 2021. "Dynamics of a Nonlinear Energy Harvester with Subharmonic Responses." *Journal of Physics: Conference Series* 1736(1). ISSN: 1742-6596. DOI: 10.1088/1742-6596/1736/1/012032.

11. Margielewicz Jerzy, Damian Gąska, Grzegorz Litak, Piotr Wolszczak, Daniil Yurchenko. 2022. "Nonlinear Dynamics of a New Energy Harvesting System with Quasi-Zero Stiffness." *Applied Energy* 307: 118159. ISSN: 0306-2619. DOI: 10.1016/J.APENERGY.2021.118159.
12. Lin R. M., T.Y. Ng. 2018. "Identification of Volterra Kernels for Improved Predictions of Nonlinear Aeroelastic Vibration Responses and Flutter." *Engineering Structures* 171: 15-28. ISSN: 0141-0296. DOI: 10.1016/J.ENGSTRUCT.2018.05.073.
13. Mehdipour Iman, Francesco Madaro, Francesco Rizzi, Massimo De Vittorio. 2022. "Comprehensive Experimental Study on Bluff Body Shapes for Vortex-Induced Vibration Piezoelectric Energy Harvesting Mechanisms." *Energy Conversion and Management: X* 13: 100174. ISSN: 0196-8904. DOI: 10.1016/J.ECMX.2021.100174.
14. Zhou Zhiyong, Weiyang Qin, Pei Zhu, Wenfeng Du. 2021. "Harvesting More Energy from Variable-Speed Wind by a Multi-Stable Configuration with Vortex-Induced Vibration and Galloping." *Energy* 237: 121551. ISSN: 0360-5442. DOI: 10.1016/J.ENERGY.2021.121551.
15. Elahi Hassan, Marco Eugeni, Paolo Gaudenzi. 2022. *Galloping-Based Aeroelastic Energy Harvesting*. Elsevier. ISBN: 978-0-12-823968-1.
16. Xu Ming, Bin Wang, Xiaoya Li, Shengxi Zhou, Daniil Yurchenko. 2022. "Dynamic Response Mechanism of the Galloping Energy Harvester under Fluctuating Wind Conditions." *Mechanical Systems and Signal Processing* 166: 108410. ISSN: 0888-3270. DOI: 10.1016/J.YMSSP.2021.108410.
17. Usman Muhammad, Asad Hanif, In Ho Kim, Hyung Jo Jung. 2018. "Experimental Validation of a Novel Piezoelectric Energy Harvesting System Employing Wake Galloping Phenomenon for a Broad Wind Spectrum." *Energy* 153: 882-889. ISSN: 0360-5442. DOI: 10.1016/J.ENERGY.2018.04.109.
18. Jung Hyung Jo, Seung Woo Lee. 2011. "The Experimental Validation of a New Energy Harvesting System Based on the Wake Phenomenon." *Smart Materials and Structures* 20(5): 055022. ISSN: 0964-1726. DOI: 10.1088/0964-1726/20/5/055022.
19. Dos Santos Carlos R., Flávio D. Marques, Muhammad R. Hajj. 2019. "The Effects of Structural and Aerodynamic Nonlinearities on the Energy Harvesting from Airfoil Stall-Induced Oscillations". *Journal of Vibration and Control* 25(14): 1991-2007. ISSN: 1077-5463. DOI: 10.1177/1077546319844383.
20. Bibo Amin, Mohammed F. Daqaq. 2013. "Energy Harvesting under Combined Aerodynamic and Base Excitations." *Journal of Sound and Vibration* 332(20): 5086-5102. ISSN: 0022-460X. DOI: 10.1016/J.JSV.2013.04.009.
21. Liu Haojie, Xiumin Gao. 2019. "Vibration Energy Harvesting under Concurrent Base and Flow Excitations with Internal Resonance." *Nonlinear Dynamics* 96(2): 1067-1081. ISSN: 0924-090X. DOI: 10.1007/S11071-019-04839-4/FIGURES/15.
22. Wu Yining, Daochun Li, Jinwu Xiang, Andrea Da Ronch. 2016. "A Modified Airfoil-Based Piezoaeroelastic Energy Harvester with Double Plunge Degrees of Freedom." *Theoretical and Applied Mechanics Letters* 6(5): 244-247. ISSN: 2095-0349. DOI: 10.1016/J.TAML.2016.08.009.
23. Rajagopal Karthikeyan, Yesgat Admassu, Riessom Weldegiorgis, Prakash Duraisamy, Anitha Karthikeyan. 2019. "Chaotic Dynamics of an Airfoil with Higher-Order Plunge and Pitch Stiffnesses in Incompressible Flow." *Complexity*. Article ID 5234382. ISSN: 1076-2787. DOI: 10.1155/2019/5234382.

24. De Sousa Vagner Candido, Carlos De Marqui Junior. 2015. "Airfoil-Based Piezoelectric Energy Harvesting by Exploiting the Pseudoelastic Hysteresis of Shape Memory Alloy Springs." *Smart Materials and Structures* 24(12): 125014. ISSN: 0964-1726. DOI: 10.1088/0964-1726/24/12/125014.
25. Wei Z. A., Z.C. Zheng. 2017. "Energy-Harvesting Mechanism of a Heaving Airfoil in a Vortical Wake." *AIAA Journal* 55(12): 4061-4073. ISSN: 1533-385X. DOI: 10.2514/1.J055628.

Received 15.10.2022; accepted in revised form 02.12.2022



Scientific Journal of Silesian University of Technology. Series Transport is licensed under a Creative Commons Attribution 4.0 International License